Improvement for the hemodynamic solver, First Blood, using the MacCormack scheme

Richárd Wéber*, Márta Viharos, György Paál

Department of Hydrodynamic Systems, Faculty of Mechanical Engineering, Budapest University of Technology and Economics, Hungary

DOI: 10.17489/biohun/2024/1/594

Abstract

Numerical hemodynamic simulations can improve the diagnosis and treatment of cardiovascular-related diseases, decreasing their leading mortality. The paper presents the improvement of the hemodynamic solver, First Blood. While the method of characteristics (MOC) handles the boundary conditions, the MacCormack scheme and the MOC are also applied to solve the mass and momentum balance equations in the inner points. The Olufsen model replaces the Poynting-Thomson model to ensure the accurate modelling of the arterial wall behaviour. The study highlights the numerical superiority of the MacCormack scheme over the MOC both in accuracy and computational efficiency. The simulation of a cardiac cycle takes less than 9 seconds, while the discretisation error in the results is low. Finally, simulation results are presented to validate the physiological relevance of the solver and the applied cardiovascular model.

Keywords: hemodynamics, MacCormack, First Blood, method of characteristics

Introduction

Cardiovascular-related diseases are still among the leading causes of death in modern societies. Developing mathematical models to describe the human cardiovascular system is inevitable in increasing the quality of modern medicine. Since patient-specific treatments are spreading in general medicine, the engineering modelling can improve its accuracy with patient-specific models. This paper follows the idea of low-dimensional modelling, handling the entire cardiovascular network.

A novel hemodynamic solver, First Blood, has been recently developed, applying the method of characteristics (MOC).[1] Although the solver is both computationally efficient and accurate, there is a remarkable limitation: it cannot handle varying nominal diameters, i.e., the model cannot contain tapered artery vessels. The cerebral arteries, mainly the internal and external carotid arteries, have significant changes in their nominal diameter along the vessel. Since a varying nominal diameter highly influences the speed of the pulse wave propagation, significant modifications and

***Corresponding author contact data:** Department of Hydrodynamic Systems, Faculty of Mechanical Engineering, Budapest University of Technology and Economics, H-1111 Budapest, Műegyetem rkp. 3. **E-mail:** *rweber@hds.bme.hu* **Tel.:** +36 1 463-1690

Citation: *Wéber R, Viharos M, Paál Gy. Improvement for the hemodynamic solver, First Blood, using the MacCormack scheme. Biomech Hung. 2024;17(1):17-23.*

Received: 04/01/2024 **Accepted:** 24/05/2024

numerical improvements were necessary to overcome the issue. This paper aims at presenting the applied numerical schemes and a modified version of the MOC, while keeping the accuracy and computational efficiency.

Methods

The initial equations are the mass (*1*) and momentum (*2*) balances for incompressible fluid and a varying cross-section area[2,3]:

$$\frac{\partial A}{\partial t} + v\frac{\partial A}{\partial x} + A\frac{\partial v}{\partial x} = 0, \tag{1}$$

$$\frac{\partial v}{\partial t} + v\frac{\partial v}{\partial x} + \frac{1}{\rho}\frac{\partial p}{\partial x} + \frac{8\pi\mu}{A\rho}v = 0. \tag{2}$$

A is the cross-section area, v the velocity, ρ the density, p the pressure, μ the dynamic viscosity, x the spatial coordinate and t is the time. Since there are three unknown field variables, $A(x,t)$, $p(x,t)$ and $v(x,t)$, a third independent equation is necessary. The former version of our model1 used the viscoelastic Poynting-Thomson model but, its three independent parameters (two Young moduli and one damping factor) for each vessel are difficult to calibrate due to the lack of detailed measurement data. The Olufsen model overcomes this issue since there are only three parameters for the entire model. The cross-section area and pressure relation defines the artery wall mechanics using the Olufsen model

$$p - p_0 = \frac{1}{1-{\nu_P}^2}\frac{Eh}{r_0}\left(1-\sqrt{\frac{A_0}{A}}\right) = \\ = F\left(1-\sqrt{\frac{A_0}{A}}\right), \tag{3}$$

where the $A_0(x)$ is the nominal cross-section area, ν_P the Poisson coefficient. Moreover, the fraction with the elastic modulus E and the geometrical parameters (wall thickness h, and the nominal radius r_0) can be approximated such as

$$\frac{Eh}{r_0} = k_1 e^{k_2 r_0} + k_3, \tag{4}$$

where $k_i(i=1,2,3)$ are constants from fitting the curve to measurement points.[4] The F variable in *(3)* is introduced to simplify the calculations. The model is convenient, since it does not need additional data, all the parameters are available. Only the nominal cross-section area is necessary.

The MacCormack scheme provides a second-order accurate solution for the partial differential equation system (PDE)[5,6], *(1-3)*. However, the boundary conditions need the conversion of the PDE to ordinary differential equations (ODEs) with the MOC. The MOC creates the opportunity for defining any general boundary condition, e.g., prescribed field variable or connection with the lumped models.[7] Rearranging *(1-2)*, we get

$$\frac{\partial U}{\partial t} + M(U)\frac{\partial U}{\partial x} = S(x,t,U), \tag{5}$$

where

$$U = \begin{bmatrix} A \\ v \end{bmatrix} \tag{6}$$

and

$$M(U) = \begin{bmatrix} v & A \\ \frac{1}{\rho}\frac{\partial p}{\partial A} & v \end{bmatrix}. \tag{7}$$

Since the cross-section area might change spatially, i.e., $p=p(A(x,t), A_0(x), F(x))$, the source term is

$$S(x,t,U) = \\ = \begin{bmatrix} 0 \\ -\frac{8\pi\mu}{A\rho}v - \frac{1}{\rho}\left(\frac{\partial p}{\partial A_0}\frac{\partial A_0}{\partial x} + \frac{\partial p}{\partial F}\frac{\partial F}{\partial x}\right) \end{bmatrix}. \tag{8}$$

The eigenvalue of matrix M determines the wave speed

$$a = \sqrt{\frac{A}{\rho}\frac{\partial p}{\partial A}}, \tag{9}$$

while the transformation matrix T can be built up using the eigenvectors. Multiplying (5) from the left with T^{-1} and using $T^{-1}M=\Lambda T^{-1}$, where Λ is diagonal with the eigenvalues, we get

$$T^{-1}\frac{\partial U}{\partial t} + \Lambda T^{-1}\frac{\partial U}{\partial x} = T^{-1}S. \tag{10}$$

Introducing $T^{-1} = \partial W/\partial U$ leads, i.e.,

$$\frac{\partial W}{\partial U}\frac{\partial U}{\partial t} + \Lambda\frac{\partial W}{\partial U}\frac{\partial U}{\partial x} = T^{-1}S, \tag{11}$$

which seems a directional derivative and W the Riemann invariant; however, the nominal cross-section area changes along the vessel, $(\partial W/\partial U)(\partial U/\partial x)=(\partial W/\partial x)+C$, where C is a function of x. Finally,

$$\frac{DW}{Dt} = T^{-1}S - \Lambda C, \tag{12}$$

where D represents substantial derivatives along the lines $v\pm a$. The simple explicit Euler scheme transforms the differential equations into algebraic ones. This formula is also used to solve the equations in the inner computational points. The algebraic equations are only valid along the characteristic lines, and since the pulse wave velocity changes in time and space, linear interpolation is inevitable.

Once the Riemann invariants W have been determined, C can be calculated as well. To find the invariants, we need the definite integral of T^{-1} from a stress-free v_0, A_0 state to an arbitrary point, i.e.,

$$W_{1,2} = \frac{1}{2}(v - v_0) \pm \sqrt{\frac{2\sqrt{A_0}F}{\rho}}\left(A_0^{\frac{1}{4}} - A^{\frac{1}{4}}\right). \tag{13}$$

where the value of F is determined via (3)with geometric and material parameters. The direct spatial dependence of the invariant determines the correction C, as

$$C_{1,2} = \mp\left[\sqrt{\frac{\sqrt{A_0}}{2\rho F}}\left(A_0^{-\frac{1}{4}} - A^{-\frac{1}{4}}\right)\frac{\partial F}{\partial x} - \sqrt{\frac{F}{8\rho}}A^{-\frac{1}{4}}A_0^{-\frac{3}{4}}\frac{\partial A_0}{\partial x}\right]. \tag{14}$$

Literature provides data to build up the model for the entire cardiovascular network of the human body.[8-10] Figure 1 depicts the model with one-dimensional (1D) arteries, zero-dimensional (0D) heart, pulmonary circulation, and peripheries. While a simple RCR (resistor-capacitor-resistor) circuit models the pulmonary circulation, the 4 stage RCL circuits mimic the behaviour of the small arteries, arterioles, venules, and small veins. The system is not fully closed due to computational reasons. Calculating multiple small 0D circuits is significantly more efficient than handling them as one whole; thus, the network is cut up at the large veins. The parameters are set using literature data to obtain physiologically relevant output quantities.[1]

Results & discussion

This chapter presents the results achieved by First Blood with the improved numerical schemes. Simulation results are presented, and the MacCormack scheme and the MOC are compared in terms of accuracy and computational efficiency. The difference is only present at the update of the inner grid points, and the boundary conditions are handled with MOC in both cases. First, four different meshes are created and run to determine the necessary number of inner grid points, monitoring the computational time in seconds. Figure 2 represents the results for the MacCormack scheme (grey) and the explicit Euler with the MOC

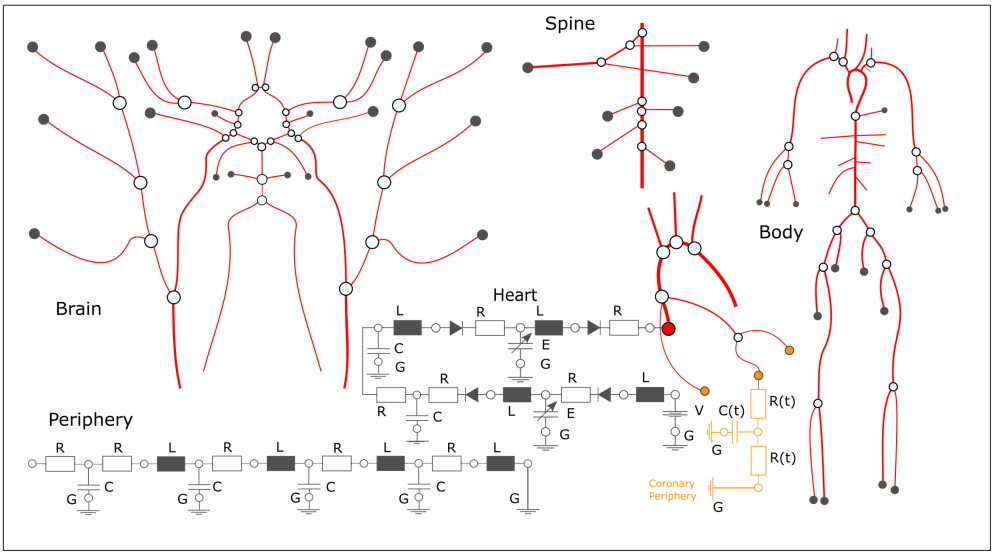

Figure 1. Illustration of the model of the entire cardiovascular network. Red lines indicate the 1D arteries, while grey circuits the peripheries, the heart, and the pulmonary circulation

(red). Second-order polynomials fit both data points accurately. Moreover, the MacCormack scheme tends to have a lower computational time as the mesh size increases.

Besides the computational time, 11 physiologically relevant diagnostic values are monitored: three diastolic, three systolic pressures from the radial, the aortic and the carotid arteries, four different pulse wave velocities, and the cardiac output. *Figure 3* presents the results as a function of the mesh size, the red being the MacCormack, and the grey the method of characteristics. Power-law functions fit the data points accurately. All plots indicate the accuracy benefit of the MacCormack method, as even the second smallest mesh could achieve sufficiently accurate results, while the MOC needs the largest mesh to be four times larger. The MacCormack method is second-order both in time and space, explaining its advantages.

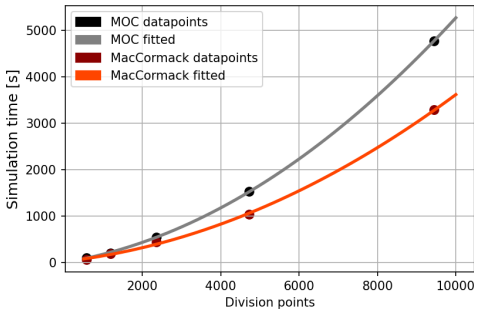

Figure 2. Simulation time as a function of the mesh size (number of grid points). MOC represents the explicit Euler scheme with the method of characteristics

Finally, since the accuracy-efficiency analysis highlighted the advantages of the MacCormack method, its simulation results are presented. *Figure 4* depicts simulation results with the pressure and the volumetric flow rate from different locations of the human body. The aortic pressure might be the most important in terms of diagnosis. Both the range and the signal shape are physiologically relevant. Also, the aortic flow rate indicates the cardiac output. The increment of the ventricular pressure opens the aortic valve, introducing a high flow rate to the aorta. However, once the elastance

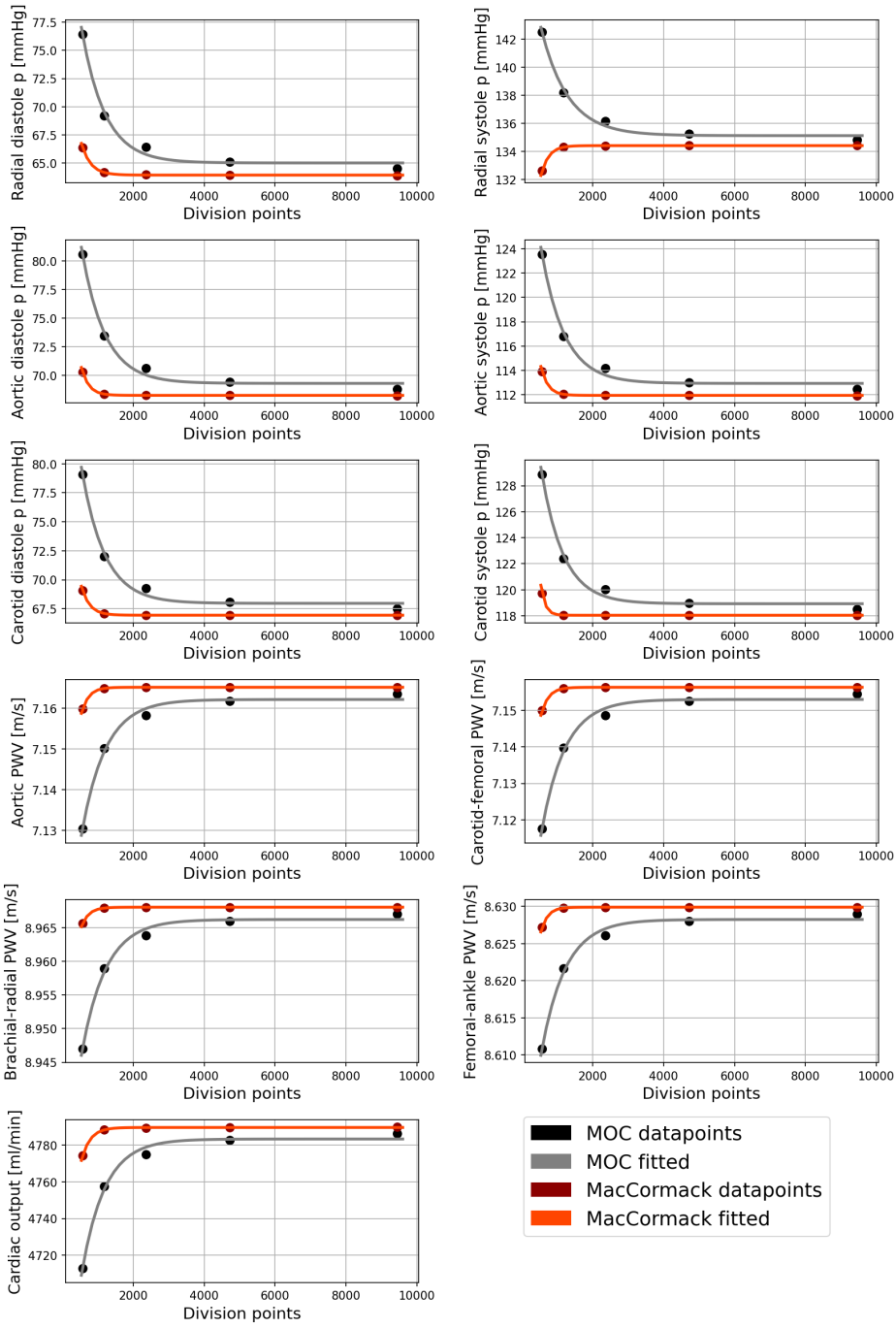

Figure 3. Physiologically relevant diagnostic outputs from both simulations using the MacCormack scheme and the method of characteristics, indicating the superiority of the former

decreases, the valve closes, stopping the velocity as well. As moving away from the aorta, the pressure amplitudes are higher and shifted in time since the vessels are elastic, and the pulse wave velocities are in the range of 5-10 m/s.[11]

Conclusion

The paper presented the numerical accuracy and computational efficiency improvements for the First Blood hemodynamic solver. After introducing the implementation of the MOC for the solution of the mass and momentum balance equations at the boundary conditions, both the MacCormack scheme and the MOC were applied to achieve results in the inner computational points. The study highlighted the superiority of the MacCormack scheme both in terms of accuracy and CPU time. A cardiac cycle requires only 9 seconds, while the discretisation error remains low. Finally, simulation results showed relevant physiological output quantities, such as aortic pressure, cardiac output or pulse wave velocity.

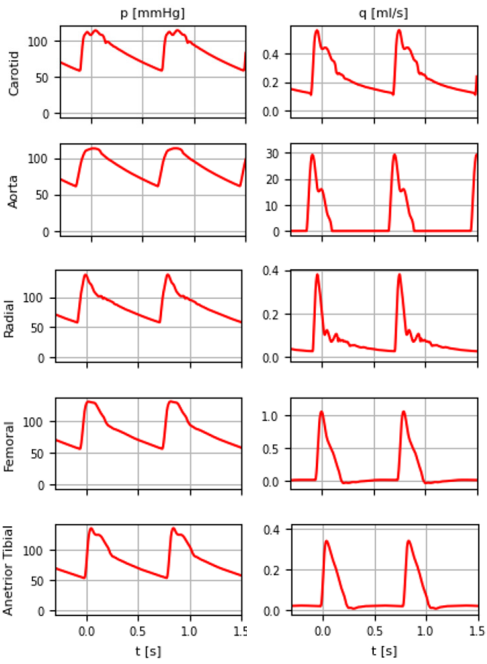

Figure 4. Pressure (p) and volumetric flow rate (q) results from five different locations of the cardiovascular network using the MacCormack scheme

Author contributions: R.W.: literature review, programming, manuscript writing, M.V.: programming, simulations, manuscript writing, figures, P.G.: research leader, feedback on manuscript.

Acknowledgements: This study was supported by the European Commission through the H2020 project "In Silico World: Lowering barriers to ubiquitous adoption of In Silico Trials" (topic SC1-DTH-06-2020, grant ID 101016503).

The research was supported by the János Bolyai Research Scholarship (BO/00484/23/6) of the Hungarian Academy of Sciences and by the New National Excellence Program of the Ministry for Culture and Innovation from the source of the National Research (Wéber Richárd ÚNKP-22–5-BME-426).

Project no. TKP-6-6/PALY-2021 has been implemented with the support provided by the Ministry of Culture and Innovation of Hungary from the National Research, Development and Innovation Fund, financed under the TKP2021-EGA funding scheme.

Conflict of interest: None.

References

1. *Wéber R, Gyürki D, Paál G. First blood:* An efficient, hybrid one- and zero-dimensional, modular hemodynamic solver. Int J Numer Method Biomed Eng 2023. DOI
2. *Mynard JP, Smolich JJ.* One-dimensional haemodynamic modeling and wave dynamics in the entire adult circulation. Ann Biomed Eng 2015;43:1443–60. DOI
3. *Ghitti B, Blanco PJ, Toro EF, Müller LO.* Construction of hybrid 1D-0D networks for efficient and accurate blood flow simulations. Int J Numer Methods Fluids 2022. DOI
4. *Olufsen MS.* Structured tree outflow condition for blood flow in larger systemic arteries. 1999.
5. *Saito M, Ikenaga Y, Matsukawa M, Watanabe Y, Asada T, Lagrée PY.* One-dimensional model for propagation of a pressure wave in a model of the human arterial network: Comparison of theoretical and experimental results. J Biomech Eng 2011;133. DOI
6. *Hellevik LR, Vierendeels J, Kiserud T, Stergiopulos N, Irgens F, Dick E, et al.* An assessment of ductus venosus tapering and wave transmission from the fetal heart. Biomech Model Mechanobiol 2009;8:509–17. DOI
7. *Formaggia L, Lamponi D, Tuveri M, Veneziani A.* Numerical modeling of 1D arterial networks coupled with a lumped parameters description of the heart. Comput Methods Biomech Biomed Engin 2006;9:273–88. DOI
8. *Reymond P, Merenda F, Perren F, Rüfenacht D, Stergiopulos N.* Validation of a one-dimensional model of the systemic arterial tree. Am J Physiol Heart Circ Physiol 2009;297:208–22. DOI
9. *Sankaran S, Moghadam ME, Kahn AM, Tseng EE, Guccione JM, Marsden AL.* Patient-specific multiscale modeling of blood flow for coronary artery bypass graft surgery. Ann Biomed Eng 2012;40:2228–42. DOI
10. *Kim HJ, Vignon-Clementel IE, Coogan JS, Figueroa CA, Jansen KE, Taylor CA.* Patient-specific modeling of blood flow and pressure in human coronary arteries. Ann Biomed Eng 2010;38:3195–209. DOI
11. *Charlton PH, Harana JM, Vennin S, Li Y, Chowienczyk P, Alastruey J.* Modeling arterial pulse waves in healthy aging: a database for in silico evaluation of hemodynamics and pulse wave indexes. Am J Physiol Heart Circ Physiol 2019;317:H1062–85. DOI